Available online at www.sciencedirect.com
SCIENCE DIRECT®

Journal of the European Ceramic Society 23 (2003) 3113–3117
www.elsevier.com/locate/jeurceramsoc

Mullite single crystal fibres produced by the internal crystallization method (ICM)

C.H. Rüscher[a,*], S.T. Mileiko[b], H. Schneider[c]

[a]Department of Mineralogy and Center for Solid State Chemistry and New Materials (ZFM), Hannover University, Welfengarten 1, D-30167 Hannover, Germany
[b]Solid State Physics Institute of the Russian Academy of Sciences, Cherenogolovka, Moscow District, 142432, Russia
[c]German Aerospace Center (DLR), Institute of Materials Research, D-51147 Köln, Germany

Received 1 September 2002; accepted 22 February 2003

Abstract

Optically clear, inclusion-free mullite fibers up to 80 mm in length and 80×70 μm^2 in cross-section were grown from an alumino silicate melt by the internal crystallization method (ICM). Microprobe analysis reveals a high chemical homogeneity at 76.5 ± 0.5 wt.% Al_2O_3 and 23.5 ± 0.5 wt.% SiO_2, which is close to the 2/1-mullite composition. Areas of slightly decreased Al_2O_3 content (≈74.5 wt.%) occur rarely, whereas areas of increased Al_2O_3 content were not observed. Polarized infrared-reflection micro-spectroscopy using spot sizes of 60 μm diameter on sections cut parallel and perpendicular to the fiber axis show the single crystal character of the fibers. Optical microscopy shows that the fibers consist of a mosaic of single crystal areas up to about 5 mm in length. The *c* axis of the single crystal individuals are misalligned up to $\theta \approx \pm 3^\circ$ with respect to the fiber axis. These orientational misfits are believed to be the reason for the development of the mosaic type microstructure during the growth process.

Keywords: Crystals; Fibres; Internal crystallisation method; Mullite

1. Introduction

Ceramic fibers exhibiting long-term high temperature stability, low creep, high strength and high oxidation resistance are key requirements for ceramic matrix composites for use in thermal protection systems (TPS) for gas turbine engines, re-entry space vehicles and similar demanding applications.[1] Oxide fibers with sufficient thermomechanical stability have high potential for these applications. Different types of commercial fibers with alumina (e.g. 3M Nextel 610) or near mullite composition (e.g. 3M Nextel 720 and Sumitomo Altex) have been used to reinforce oxide matrices. These polycrystalline oxide fibers display grain coarsening and non-elastic deformation at elevated temperatures[2–4] which is caused by the relatively strong cation and oxygen diffusion in oxides especially along grain boundaries. A possible way to overcome these problems is to use single crystal fibers made by pulling from oxide melts with subsequent crystallization.[5–7] An alternative fiber preparation technique, the so called internal crystallization method (ICM)[8,9] was developed initially to produce molybdenum fiber/oxide-matrix composites.[8] Later on the technique was modified to produce single crystalline and eutectic oxide fibers.[10,11] The ICM makes use of a molybdenum former with thousands of parallel channels. According to this technique thousands of single crystal fibers can be produced simultaneously in a low cost process. The present paper reports results of a systematic characterization of ICM mullite single crystal fibers using X-ray diffractiometry, microprobe analysis, microprobe and optical spectroscopy together with polarized infared (IR) reflection micro spectroscopy.

2. Fiber growth and methods of characterization

The fibers were produced by using the internal crystallization method (ICM).[8–11] The ICM technique includes the following steps (Fig. 1):

* Corresponding author.
E-mail address: c.ruescher@mineralogie.uni-hannover.de (C.H. Rüscher).

0955-2219/03/$ - see front matter © 2003 Elsevier Ltd. All rights reserved.
doi:10.1016/S0955-2219(03)00118-3

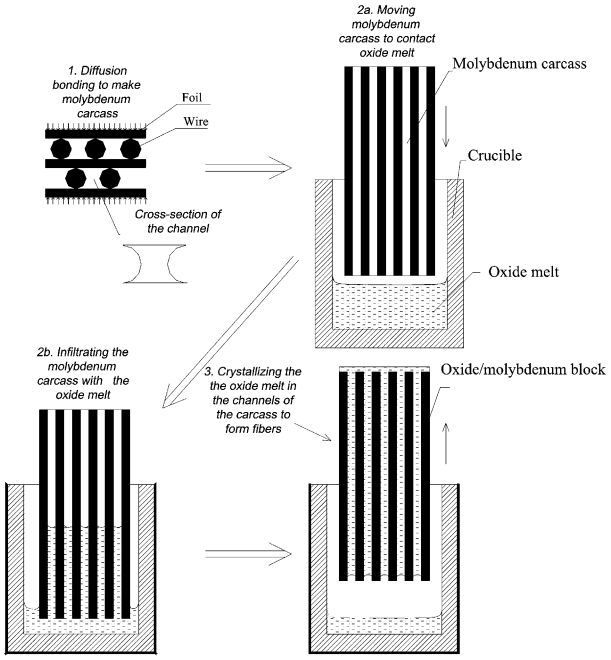

Fig. 1. Schematic view of the ICM (Internal Crystallisation Method) mullite fiber production route.

- The molybdenum former contained cylindrical channels and was obtained by diffusion welding of an assemblage of molybdenum wires and foils.
- For the production of the fibers a raw mullite precursor material were made by reaction sintering of a mixture of Al_2O_3 and SiO_2 powders. The precursor materials were molten at 1900 °C in a molybdenum crucible and the molybdenum former was then placed into the crucible in sufficient contact to the melt. The melt was infiltrated by capillary forces within about 10 min into the channels of the molybdenum former.
- In order to crystallize the mullite fiber the oxide/molybdenum block was pulled with a rate of 2 mm/min to the cold zone of the furnace.
- In the final step the extraction of the fibers was achieved by dissolving the matrix in inorganic acid.

The lengths of the as grown fibers move up to about 8 cm. Typical crossections are as shown in Fig. 2. The outer shape of these fibers is given by the molybdenum former (70×80 μm). X-ray diffraction investigations were carried out on selected powdered fibers using about 2 mg sample for Guinier photographs (Si as internal standard) and sufficient material for standard diffractometer pattern (Philips PW 1800). Some fibers were glued with their fiber axis parallel to the face of the slide and then abraded and polished to a thickness of

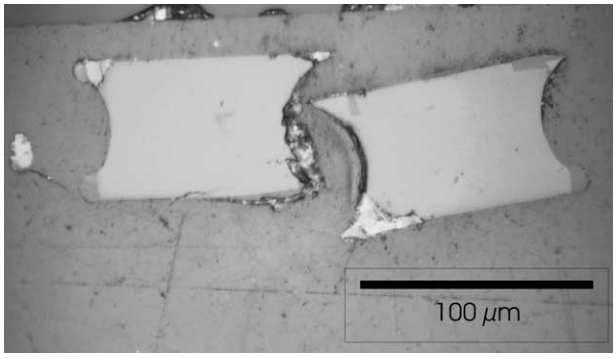

Fig. 2. Typical crossections of mullite fibers as used for micro-spectroscopical investigations (optical microscope in reflection mode).

35 μm. These samples were investigated by microprobe analysis (Cameca), polarization microscopy and by polarized IR-reflection micro spectroscopy with spot sizes of 60 μm (Bruker IFS88/microscope/KRS5 polarizer/Al-mirror as reference). Other fibers were glued with the fiber axis perpendicular to the slide face of the holder, abraded, polished and then investigated by polarized IR reflection micro spectroscopy. Details of this method were described recently by Rüscher.[12]

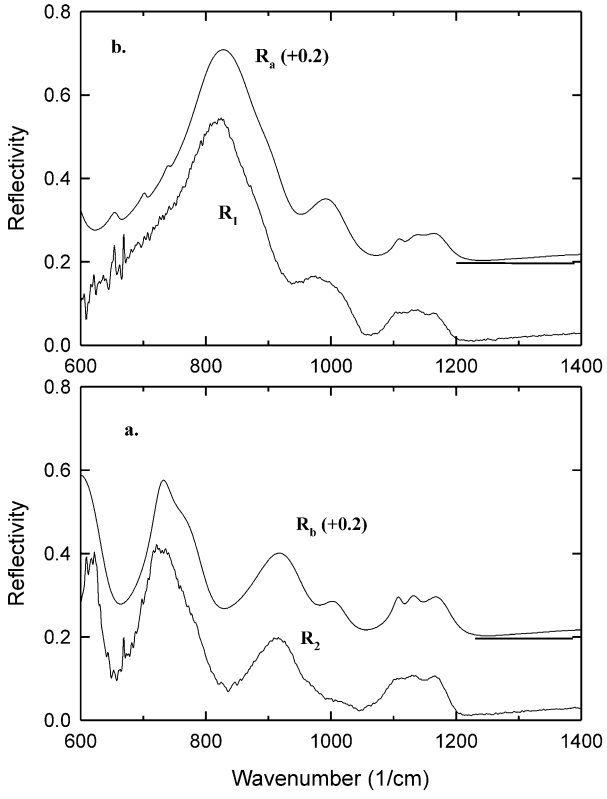

Fig. 3. Main reflectivities R_1, R_2 of fiber crosssection at normal incidence and corresponding single crystal spectra R_a, R_b calculated according to data given in Ref. 15 (shifted as denoted for clarity).

3. Results and discussion

X-ray diffraction (Guinier method) of two powdered fibers showed single phase mullite. The refined lattice parameters [$a = 0.7580(2)$ nm, $b = 0.7685(2)$ nm, $c = 0.28859(6)$ nm] are consistent with those of 2/1-mullite. Traces of α-Al_2O_3 were detected using a larger number of powdered fibers in the X-ray diffractometer pattern.

Results of micropobe analysis of the mullite fibers using a step scan technique over a distance of 3400 μm in steps of 50 μm along the fiber and in 5 μm steps transversely reveal an excellent chemical homogeneity. The obtained chemical composition is on average 76.5±0.5 wt.% Al_2O_3 and 23.5±0.5 wt.% SiO_2 close to the ideal composition of 2/1 mullite (78 wt.% Al_2O_3, 22 wt.% SiO_2).[13] A few measurement spots yielded an increased SiO_2 content up to about 74.5 wt.% Al_2O_3 and 25.5 wt.% SiO_2. These compositional variations could be attributed to some inhomogeneities in the melt. On the other hand Al_2O_3-inclusions or Al_2O_3 enriched areas were not detected by microprobe analysis.

Eight crossections of different fibers (Fig. 2) were investigated by polarized reflection spectroscopy. All of them display spectra as shown in Fig. 3. By rotating the specimens the spectra vary according to the standard relation[14]

$$R(\varphi) = R_1\cos^2(\varphi) + R_2\sin^2(\varphi). \quad (1)$$

The spectra R_1 and R_2 are in agreement with the reflectivities of the main direction R_a and R_b of 2:1 mullite[15] as shown in Fig. 3. The triplicate peak structure between 1100 and 1200 cm^{-1} may be noted. The similar intensity of these peaks differentiates the composition of the fiber from other mullite compositions, e.g. from 3:2-mullite.[12] It turns out that the a (R_a) and b (R_b) axis of mullite run approximately along the diagonals of the typical contours of the fiber crossections. Representative spectra of the fibers using micro spectroscopic analyses (spot size: 60 μm diameter) with the electrical field

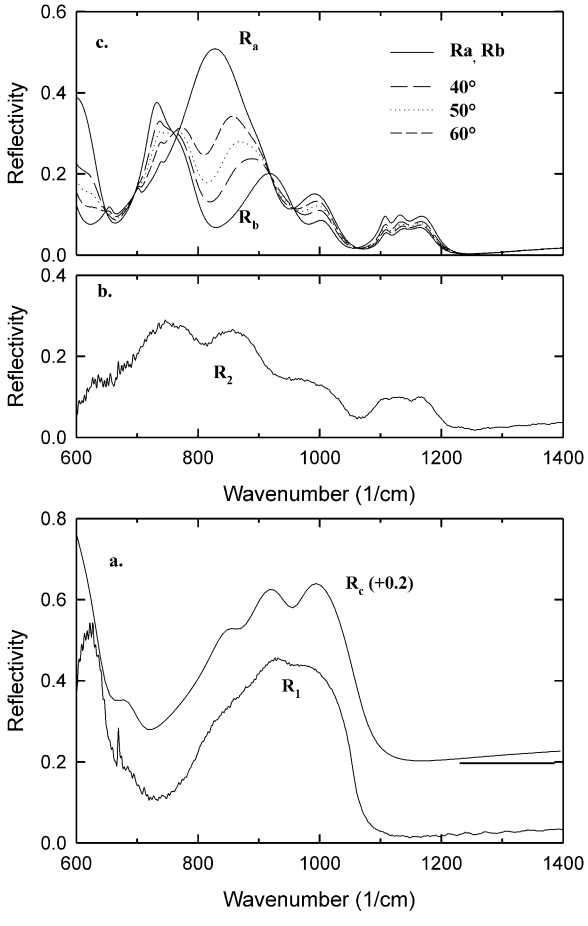

Fig. 4. Typical reflectivities for the electrical field parallel (a) and perpendicular (b) to the fiber axis at normal incidence for cuts parallel to the fiber growth (compare Fig. 5). Calculated spectra using data given in Ref. 15 are given for R_c (a) and for R_a, R_b and for cuts of 40°, 50°, 60° of the a axis with respect to the cutting surface (c). Details are described in the text.

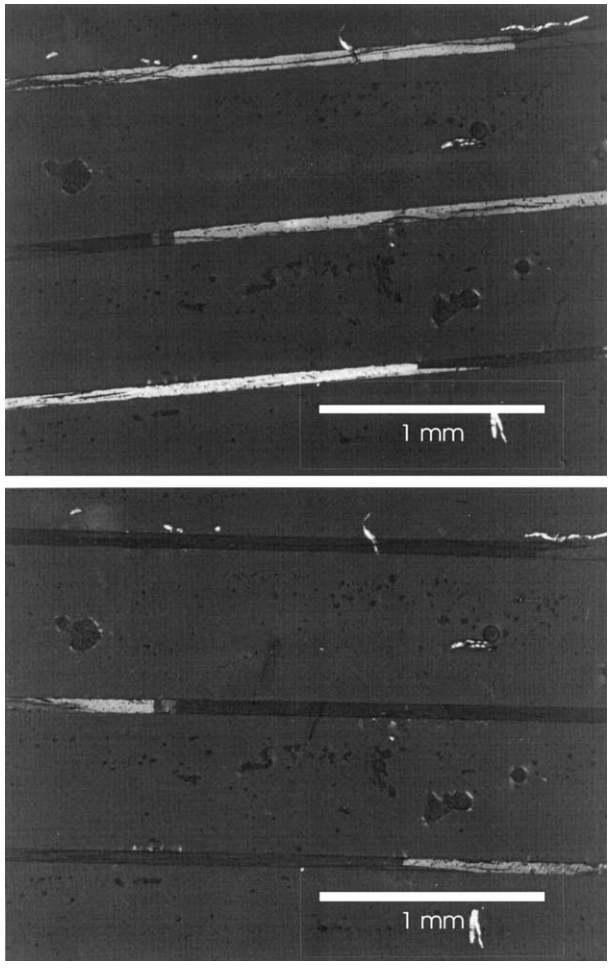

Fig. 5. Thin section micrographs of the fibers as observed under crossed polarizers in the optical microscope. Shown is the exsolution of adjacent areas of the fibers rotated by about +2.5° (top) and −2.5° (bottom) of the fiber axis with repect to the polarised orientation of the microscope.

(E) polarized parallel and perpendicular to the fiber axis are given in Fig. 4. All spectra obtained with E parallel to the fiber axis are in excellent agreement with results of single crystal mullite for E//c polarisation.[15] For E perpendicular to the fiber axis the spectra are also in good agreement with calculated spectra using dielectric functions for E//a and E//b for 2/1-mullite[15] based on elemental crystal optics[16] (see Appendix, Fig. 4c).

Thin section optical microscopy using crossed polarizers shows that the fibers consist of individual single crystal areas (Fig. 5). The length of the single crystal areas vary in a wide range up to some millimeter in length with sharp interfaces between adjacent individuals. At these interfaces the exsolution alignment jumps up to 6° from one single crystal area to the other, i.e. up to ±3° with respect to the fiber axis. However, polarized IR-reflection microspectroscopy display no significant distinction in the spectra of adjacent fragments.

The bending strength characteristics of the fibers show a significant increase for fiber lengths below about 5 mm.[17] This indicates an intrinsic bending strength of these single crystal mullite fibers, which is correlated with "undistorted" single crystal areas. On the other hand the decrease of bending strength of fibers longer than about 5 mm may be controlled by the occurrence of interfaces between two adjacent single crystal areas. A better alignment of the crystallographic *c* axis parallel to the fiber axis avoiding such bicrystal interfaces may thus help to improve significantly the mechanical properties of the ICM fibers.

Acknowledgements

The authors thank O. Diedrich for preparing thin sections, Dr. J. Koepke for carrying out the microprobe analysis, M. Kleinod for measurements of IR reflection micro spectra during his Bachelor work and an unknown referee for valuable comments.

Appendix

These reflection spectra can be calculated using the Fresnel equation for the dielectric function as $R(\theta)_{(ab)} = Z/N$, with:

$$Z = 1 + \left(\varepsilon'^2 + \varepsilon''^2\right)^{0.5} - \left(\left(\varepsilon'^2 + \varepsilon''^2\right)^{0.5} + 2\varepsilon'\right)^{0.5} \quad \text{and}$$

$$N = 1 + \left(\varepsilon'^2 + \varepsilon''^2\right)^{0.5} + \left(\left(\varepsilon'^2 + \varepsilon''^2\right)^{0.5} + 2\varepsilon'\right)^{0.5}.$$

Here the real and imaginary part of the effective dielectric function, $\varepsilon_{\text{eff}} = \varepsilon' + i\varepsilon''$, for crystal cut with angle Θ for the tensor components between $\Theta = 0°$ ($\varepsilon_a = \varepsilon_a' + i\varepsilon_a''$) and $\Theta = 90°$ ($\varepsilon_b = \varepsilon'_b + i\varepsilon_b''$) is given by $1/(\varepsilon_{\text{eff}}) = \cos^2(\Theta)/\varepsilon_{\text{a}} + \sin^2(\Theta)/\varepsilon_{\text{b}}$ as $\varepsilon' = AB/(B^2 + C^2)$, $\varepsilon'' = AC/(B^2 + C^2)$ using the abbreviations:

$$A = \left(\varepsilon_a'^2 + \varepsilon_a''^2\right), \left(\varepsilon_b'^2 + \varepsilon_b''^2\right)$$

$$B = \left(\varepsilon_b'\right)\left(\varepsilon_a'^2 + \varepsilon_a''^2\right)\sin^2(\theta) + \left(\varepsilon_a'\right)\left(\varepsilon_b'^2 + \varepsilon_b''^2\right)\cos^2(\theta)$$

$$C = \left(\varepsilon_b''\right)\left(\varepsilon_a'^2 + \varepsilon_a''^2\right)\sin^2(\theta) + \left(\varepsilon_a''\right)\left(\varepsilon_b'^2 + \varepsilon_b''^2\right)\cos^2(\theta)$$

The spectra ε_a and ε_b of the main polarisations for E//a and E//b are calculated using values for single crystal 2:1 mullite[15] with Lorentzian peaks:

$$\varepsilon(w) = \varepsilon_\infty + \Sigma_n\left(F_n w_{\text{Tn}}^2\right)\left(w_{\text{Tn}}^2 - w^2\right)/\left(\left(w_{\text{Tn}}^2 - w^2\right)^2 + y_n^2 w^2\right) + i\left(F_n w_{\text{Tn}}^2 y_n w\right)/\left(\left(w_{\text{Tn}}^2 - w^2\right)^2 + y_n^2 w^2\right)$$

References

1. Schneider, H., Göring, J., Kanka, B. and Schmücker, M., Whipox: ein neuer Oxidfaser/Oxidmatrix-Leichtbauwerkstoff für Hochtemperaturanwendungen. *Keram. Z.*, 2001, **53**, 788–791.
2. Schneider, H., Göring, J., Schmücker, M. and Flucht, F., Thermal stability of Nextel 720 alumino-silicate fibers. In *Ceramic Microstructures: Control at Atomic Level*, ed. A. P. Tomsia and A. M. Glaeser. Plenum Press, New York, 1998, pp. 721–730.
3. Schmücker, M., Kanka, B. and Schneider, H., Mesostructure of WHIPOX™ all oxide ceramics. In *High Temperature Ceramic Matrix Composites*, ed. W. Krenkel, R. Naslain and H. Schneider. Wiley VCH, 2001, pp. 670–674.
4. Braue, W., Borath, R., Flucht, F. and Schneider, H., Failure analysis of Nextel™ 720 fibers subjected to high-temperature testing: The role of intrinsic fiber impurities. In *High Temperature Ceramic Matrix Composites*, ed. W. Krenkel, R. Naslain and H. Schneider. Wiley VCH, 2001, pp. 90–95.
5. Kriven, W. M., Jilavi, M. H., Kim, D., Weber, J. K. R., Cho, B., Telten, J. J. and Nordine, P. C., Synthesis and microstructure of mullite fibers grown from deeply undercooled melts. In *Ceramic Microstructures: Control at Atomic Level*, ed. A. P. Tomsia and A. M. Glaeser. Plenum Press, New York, 1998, pp. 170–176.
6. Weber, J. K. R., Cho, B., Hixsan, A. D., Abadie, J. G., Nordine, P. C., Kriven, W. M., Johnson, B. R. and Kim, D., Growth and crystallisation of YAG- and mullite composition glass fibers. *J. Eur. Ceram. Soc.*, 1999, **19**, 2543–2550.
7. Sayir, A. and Farmer, S. C., Directionally solidified mullite fibers, Ceramic matrix composites advanced high-temperature structural materials.
8. Mileiko, S. T. and Kazmin, V. I., Crystallization of fibres inside a matrix: a new way of fabrication of composites. *J. Mater. Sci.*, 1992, **27**, 2165–2172.
9. Mileiko, S. T. and Kazmin, V. I., Structure and mechanical properties of oxide fibre reinforced metal matrix composites produced by the internal crystallization method. *Comp. Sci. Technol.*, 1992, **45**, 209–220.
10. Mileiko, S. T., Kiiko, V. M., Sarkissyan, N. S., Starostin, M. Yu.,

Gvozdeva, S. I., Kolchin, A. A. and Strukova, G. K., Microstructure and properties of Al_2O_3–$Al_5Y_3O_{12}$ fibre produced via internal crystallization route. *Comp. Sci. Technol*., 1999, **59**, 1763–1772.

11. Kurlov, V. N., Kiiko, V. M., Kolchin, A. A. and Mileiko, S. T., Sapphire fibres grown by a modified internal crystallization method. *J. Cryst. Growth*, 1999, **204**, 499–504.
12. Rüscher, C. H., Thermic transformation of sillimanite single crystals to 3:2 mullite plus melt: investigations by polarized IR-reflection micro spectroscopy. *J. Eur. Cer. Soc*., 2001, **21**, 2463–2469.
13. Schneider, H., Okada, K. and Pask, J. A., *Mullite and Mullite Ceramics*. John Wiley and Sons, 1994, 1–251.
14. Raabe, H., Die Erkennung und quantitative Datenerfassung optischer Hauptschnitte von stark absorbierenden, anisotropen Kristallen mit dem Auflicht-Polarisationsmikroskop. *Fortschr. Miner*., 1983, **61**, 243–281.
15. Rüscher, C. H., Phonon spectra of 2:1 mullite in infrared and Raman experiments. *Phys. Chem. Min*., 1996, **23**, 50–55.
16. Born, M. and Wolf, E., *Principles of Optics*, 6th edn. Pergamon Press, 1980, 1–808, Chapter XIV.
17. Mileiko, S. T., Kiiko, V. M., Starostin, M.Yu, Kolchin, A. A. and Kozhevnikov, L. S., Fabrication and some properties of single crystalline mullite fibers. *Scripta Materialia*, 2001, **44**, 249–255.